JACS
JOURNAL OF THE AMERICAN CHEMICAL SOCIETY

ARTICLE

pubs.acs.org/JACS

Reversible Photoredox Switching of Porphyrin-Bridged Bis-2,6-di-*tert*-butylphenols

Shinsuke Ishihara,[†] Jonathan P. Hill,[*,†,‡] Atsuomi Shundo,[†] Gary J. Richards,[◇] Jan Labuta,[†] Kei Ohkubo,[§,▽] Shunichi Fukuzumi,[§,▽,∥] Akira Sato,[⊥] Mark R. J. Elsegood,[#] Simon J. Teat,[¶] and Katsuhiko Ariga[*,†,‡]

[†]WPI Research Center for Materials Nanoarchitectonics, National Institute for Materials Science, 1-1 Namiki, Tsukuba, Ibaraki 305-0044, Japan

[‡]JST, CREST, 1-1 Namiki, Tsukuba, Ibaraki 305-0044, Japan

[◇]Fuel Cell Materials Center, National Institute for Materials Science, 1-1 Namiki, Tsukuba, Ibaraki 305-0044, Japan

[§]Department of Material and Life Science, Graduate School of Engineering, Osaka University, 2-1 Yamadaoka, Suita, Osaka 565-0871, Japan

[▽]JST, ALCA, 2-1 Yamadaoka, Suita, Osaka 565-0871, Japan

[∥]Department of Bioinspired Science, Ewha Womans University, Seoul 120-750, Korea

[⊥]Materials Analysis Station, National Institute for Materials Science, 1-1 Namiki, Tsukuba, Ibaraki 305-0044, Japan

[#]Chemistry Department, Loughborough University, Loughborough, Leicestershire LE11 3TU, U.K.

[¶]ALS, Berkeley Lab, 1 Cyclotron Road, MS2-400, Berkeley, California 94720, United States

Supporting Information

ABSTRACT: Porphyrin derivatives bearing 2,6-di-*tert*-butylphenol substituents at their 5,15-positions undergo reversible photoredox switching between porphyrin and porphodimethene states as revealed by UV−vis spectroscopy, fluorescence spectroscopy, and X-ray single-crystal analyses. Photoredox interconversion is accompanied by substantial variations in electronic absorption and fluorescence emission spectra and a change of conformation of the tetrapyrrole macrocycle from planar to roof-shaped. Oxidation proceeds only under photoillumination of a dianionic state prepared through deprotonation using fluoride anions. Conversely, photoreduction occurs in the presence of a sacrificial electron donor. Transient absorption spectroscopy and electron spin resonance spectroscopy were applied to investigate the processes in photochemical reaction, and radical intermediates were characterized. That is, photooxidation initially results in a phenol-substituent-centered radical, while the reduction process occurs via a delocalized radical state involving both the macrocycle and 5,15-substituents. Forward and reverse photochemical processes are governed by different chemical mechanisms, giving the important benefit that conversion reactions are completely isolated, leading to better separation of the end states. Furthermore, energy diagrams based on electrochemical analyses (cyclic voltammetry) were used to account for the processes occurring during the photochemical reactions. Our molecular design indicates a simple and versatile method for producing photoredox macrocyclic compounds, which should lead to a new class of advanced functional materials suitable for application in molecular devices and machines.

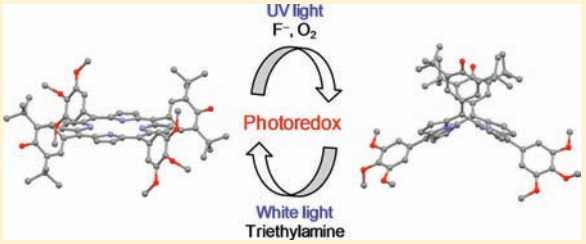

INTRODUCTION

Design of functional porphyrin and porphyrinoid analogues is a subject of great current interest due to their optoelectronic,[1] magnetic,[2] catalytic,[3] and self-assembling[4] properties. Porphyrins are considered of special significance because of the possibility of coupling their various redox states with different optical states or for physical coupling with other chromophores, leading to important phenomena including optical switching[5] and charge separation.[6] Furthermore, porphyrin hybrids containing quinonoid,[7] TCNQ,[8] C_{60},[9] or ketone[10] structural features have been reported. These systems possess redox and photochemical properties that vary from those of conventional porphyrins. Porphyrins bearing phenolic[5,6,11] (or hydroxylic[5,6a,11]) substituents are known to undergo structural changes depending on their states of protonation and relative susceptibilities to oxidation, which can be further compounded with tautomeric processes,[12] and which bear some similarities with the reversible hydroquinone/quinone redox system.[13] Previously, we reported redox switching based on fluoride-anion-triggered redox interconversion of porphyrin derivatives.[5] In that case, 5,10,15,20-tetrakis(3,5-di-*tert*-butyl-4-hydroxyphenyl)porphyrin [T(DtBHP)P] underwent fluoride-anion-triggered aerial oxidation, whereas 5,15-bis(3,5-di-*tert*-butyl-4-hydroxyphenyl)-10,20-diphenylporphyrin [D(DtBHP)P] did not. Also, the removal of fluoride anion and subsequent addition of ascorbic acid returned T(DtBHP)P to its original state.

Received: June 28, 2011
Published: August 29, 2011

In this way, a chemically operated memory system could be demonstrated.

However, there have been only a few reports of porphyrin or multichromophore systems undergoing reversible photochemically coupled reactions between states having discrete electronic absorptive *and* differing structural conformations. With this in mind, light would make an ideal stimulus for triggering electrochemical or morphological changes in molecules because it is highly energetic and enables manipulation of molecules with precise time−space resolution.[14] There are also a variety of recently proposed technologies aimed at overcoming the diffraction limit of light, which would enable the manipulation of molecules (or assemblies of molecules) using light.[15] Thus, we considered the design of a porphyrin−hydroquinone hybrid to demonstrate reversible *photoredox* interconversion between reduced and oxidized states of the porphyrin. Despite the existence already of a few photoredox systems, no examples have been reported in which the end products of photoredox conversion have been isolated and fully characterized. Considering the substantial variation in molecular properties available through hybridization of porphyrins, the dynamic interconversion between two states of some archetypal molecule, such as a porphyrin−hydroquinone hybrid, provides a potential means for developing photoresponsive molecular devices.[16]

Here we show that 5,15-bis(3,5-di-*tert*-butyl-4-hydroxyphenyl)-substituted porphyrins can be operated as reversible photochemical molecular switches. Porphyrin **1** bearing such groups at its 5,15-positions undergoes photoinduced aerial oxidation to porphodimethene **2** with drastic variations of both electronic and conformational structures, as demonstrated by UV−vis absorption spectroscopy, fluorescent spectroscopy, and X-ray single-crystal analyses. Moreover, **2** undergoes a photoinduced reduction, reverting to **1** in the presence of a sacrificial electron donor, in this case triethylamine (TEA). Forward (**1**→**2**) and reverse (**2**→**1**) processes are governed by different chemical mechanisms, giving the important benefit that conversion reactions are completely isolated, leading to better separation (or "locking") of the end states. Thus, this photoredox system can also be recognized as a nonvolatile, nondestructive molecular memory.[5,17] To the best of our knowledge, this is the first example of a porphyrin capable of reversible photoredox interconversion.

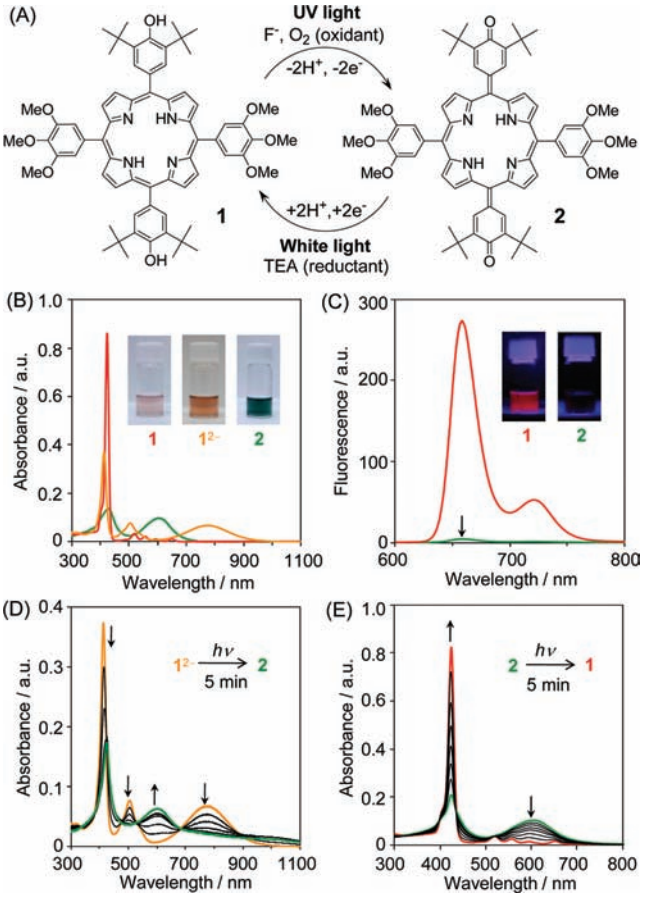

Figure 1. (A) Photoredox interconversion between porphyrin-bridged hydroquinone state **1** and quinonoid state **2**. (B) Electronic absorption spectra of **1**, $\mathbf{1}^{2-}$, and **2** (in CH_2Cl_2, 2.3×10^{-5} M). (C) Fluorescence emission spectra of **1** and **2** excited at 424 nm (in CH_2Cl_2, 1.0×10^{-6} M). The weak fluorescence peak in the spectrum of **2** (indicated by an arrow) is due to unconverted **1**. (D) Time dependence of UV-vis spectra of $\mathbf{1}^{2-}$ during UV light irradiation at 365 nm (in CH_2Cl_2, 2.3×10^{-5} M, under air). (E) Time dependence of UV-vis spectra of **2** in the presence of 10^4 equiv of TEA during white light irradiation (in CH_2Cl_2, 2.3×10^{-5} M, under argon).

RESULTS AND DISCUSSION

In **1**, two 3,5-di-*tert*-butyl-4-hydroxyphenyl groups are physically coupled through the π-conjugated porphyrin ring, so that **1** bears properties of both porphyrin and hydroquinone systems. **1** is analogous with hydroquinones containing, for instance, 4,4′-dihydroxybiphenyl units since the phenyl groups are not fully electronically conjugated with the porphyrin due to steric demands. While 3,5-di-*tert*-butyl-4-hydroxyphenyl groups are used here due to the enhanced stability of their radical intermediates,[18] 3,4,5-trimethoxyphenyl groups improve the solubility of **1** in nonpolar solvents (and incidentally provide points for molecular design elaboration).

Photooxidation of **1** to **2** (Figure 1A) involves addition of a large excess of fluoride anion F^- (approximately 100 equiv as tetrabutylammonium fluoride, TBAF) to **1** in CH_2Cl_2. F^- is known to behave as a base through strong H−F hydrogen bonding, and under certain conditions F^- is known to deprotonate one pyrrolic-NH group of porphyrin, resulting in a porphyrin monoanion[19] or a hydrogen-bonded complex.[20] In the present case, mixtures of **1** and F^- exhibit an electronic absorption spectrum quite different from that of **1**, in that the absorption maximum is hypsochromically shifted and reduced in intensity, with new broad peaks appearing around 500 and 800 nm (Figure 1B). Addition of other tetrabutylammonium salts (Cl^-, Br^-, and I^-) did not cause any change in the electronic absorption spectra of **1**. The drastic change in the electronic structure of **1** in the presence of F^- is due to deprotonation of the phenol moieties (i.e., to $\mathbf{1}^{2-}$), and this is supported by X-ray crystal structure analysis and ^{1}H NMR spectroscopy of a structurally similar derivative (**3**) which lacks methoxy groups. In the crystal structure of the doubly deprotonated form of **3**, an extended array is formed involving one of the tetrabutylammonium cations, which links the phenolate substituents of the porphyrins through hydrogen bonding (see Figures 2B and 3). For $\mathbf{3}^{2-}$ in crystals, anionic charge is localized at the phenol substituents, while fluoride anions are not contained in the structure. In the case of **1**, $\mathbf{1}^{2-}$ is stable against aerial oxidation under ambient conditions, in contrast to deprotonated 5,10,15,20-tetrakis(3,5-di-*tert*-butyl-4-hydroxyphenyl)porphyrin,[5]

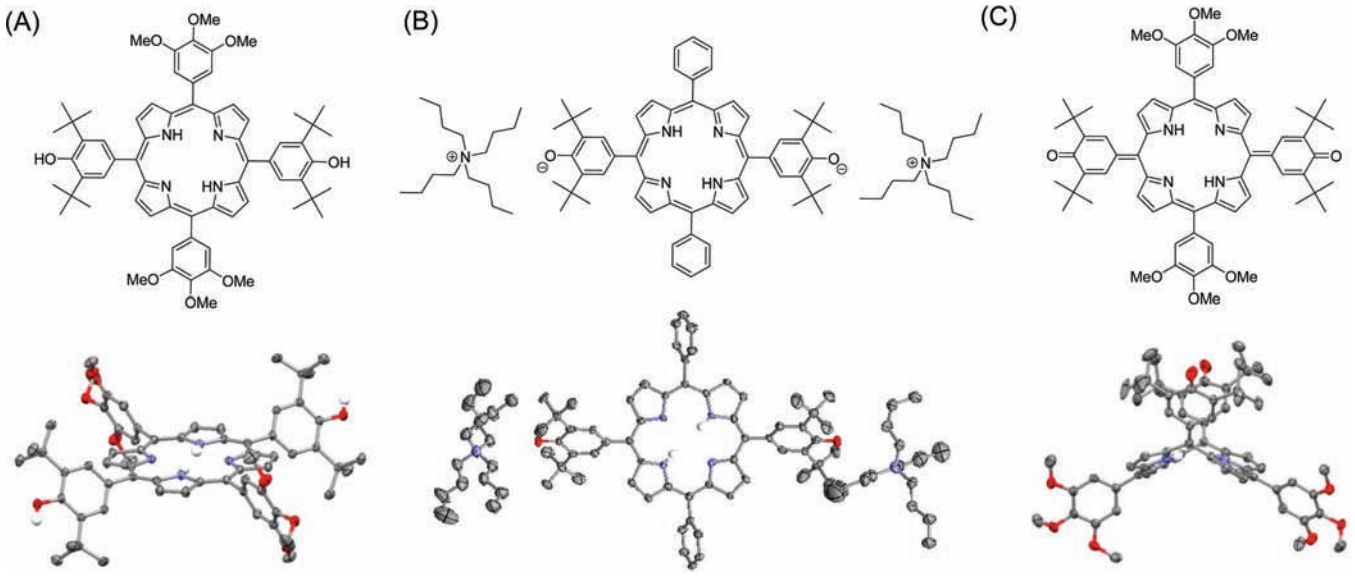

Figure 2. X-ray crystal structures of (A) **1**, (B) $\mathbf{3}^{2-}$ cocrystallized with tetrabutylammonium fluoride, and (C) **2**.[21] Porphyrin **3** is an analogue of **1** in which 3,4,5-trimethoxyphenyl groups at *meso*-positions are changed to phenyl groups. Thus, $\mathbf{3}^{2-}$ reflects the structure of $\mathbf{1}^{2-}$. Gray, carbon; blue, nitrogen; red, oxygen. The thermal ellipsoids are drawn at the 50% probability level. Solvent molecules and hydrogen atoms bound at carbon atoms are omitted for clarity. Important bond lengths and angles: C−O bond length at phenolic moiety, 1.326(2) Å (O4−C20) for **1**, 1.262(7) Å (O2−C44) for $\mathbf{3}^{2-}$, and 1.225(4) Å (O11−C58) for **2**; dihedral angle for phenolic moiety to porphyrin macrocycle, 58.9(2)° (C15−C7−C14−C9) for **1**, 49.3(8)° (C4−C5−C21−C22) for $\mathbf{3}^{2-}$, and 3.8(3)° (C12−C20−C31−C35) for **2**.

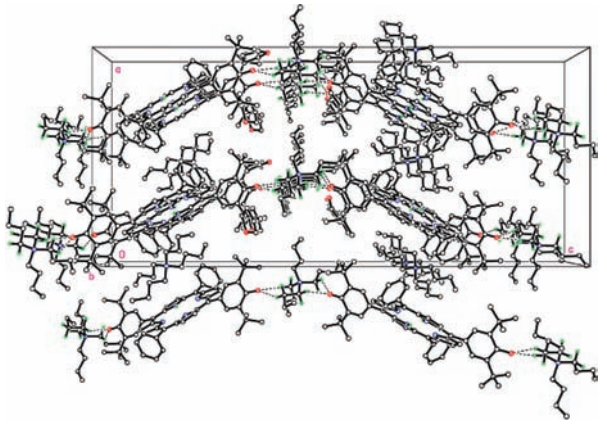

Figure 3. Crystal packing of $\mathbf{3}^{2-}$ showing the role of CH−O hydrogen bonding (3.270 Å for C81−(H89A)−O2, 3.121 Å for C81−(H81B)−O2) in forming an extended network involving one of the tetrabutylammonium cations. The remaining countercation is sandwiched between porphyrin moieties.

and removal of fluoride anions by extraction with water regenerates **1**. Resistance to oxidation is despite the fact that the first oxidation potential of **1** is decreased significantly from 0.31 V (relative to Fc/Fc^{+}) to −0.88 V on addition of F^{-} (however, it is not sufficient to permit aerial oxidation[22]).

Subsequent irradiation of **1** in the presence of F^{-} in CH_2Cl_2 with ultraviolet light (λ = 365 nm) caused an immediate color change from red to green with well-defined isosbesticity in electronic absorption spectra, and photoinduced oxidation to **2** is complete after 5 min (Figure 1D). Photoinduced oxidation does not proceed under argon atmosphere, indicating that aerial O_2 is required as an oxidant. The well-defined isosbestic point indicates that only two long-lived species are involved in this process, with the product **2** most likely existing as a fluoride anion complex (with binding of F^{-} through pyrrolic-NH).[23] Removal of F^{-} by extraction with water provides anion-free **2** and leads to a slight change in its absorption spectrum.[22] **2** is stable in solution under ambient conditions over several months, even after removal of F^{-}. Optical characteristics of **2** are quite different from those of **1** in that a broad and intense electronic absorption appears around the 600 nm region (Figure 1B), and fluorescence emission from solutions of **2** is not observed due to loss of porphyrin aromaticity (as well as intramolecular energy transfer), resulting in a large on/off ratio of fluorescence between **1** and **2** (Figure 1C).

2 can be readily toggled back to its **1** state by irradiating with white light[24] in the presence of excess TEA (as a sacrificial reductant) so that solutions regain the characteristic red color of the porphyrin macrocycle (Figure 1E). As summarized in Figure 1A, the forward (from **1** to **2**) photooxidation process requires F^{-}, O_2, and UV light irradiation, while the reverse (from **2** to **1**) requires TEA and white light irradiation. Thus, application of both chemical and photonic stimuli promotes the photoredox reactions.

Oxidation of **1** to **2** entails loss of aromaticity and an extension of conjugation over a greater number of atoms, similar to the case for the hydroquinone/quinone redox couple. However, in contrast to the hydroquinone/quinone system, the X-ray crystal structures of **1** and **2** reveal that the oxidation reaction is coupled with a serious structural change due to steric and electronic requirements (Figure 2). That is, **1** has a structure typical of other tetraphenylporphyrins[25] containing a planar tetrapyrrole macrocycle and phenyl substituents whose planes subtend an angle of ~60° with the tetrapyrrole mean plane. In strong contrast to this, **2** has a saddle-shaped structure (similar to that in ref 8 and porphodimethenes[26]), with its hemiquinone groups fully conjugated with the tetrapyrrole macrocycle, as attested to by their

dx.doi.org/10.1021/ja2056165 |*J. Am. Chem. Soc.* 2011, 133, 16119–16126

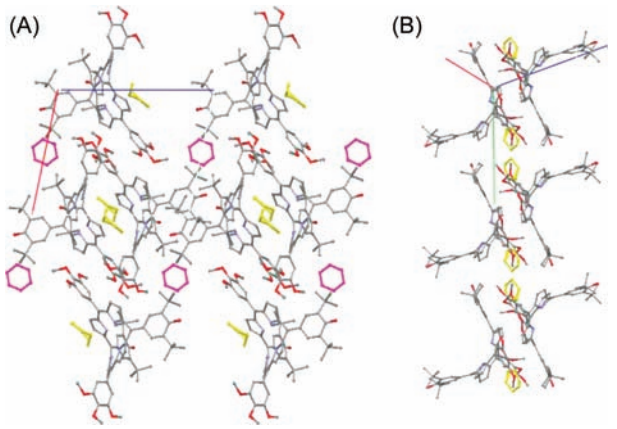

Figure 4. Crystal packing of **2**. (A) Viewed along *b*-axis. Pink and yellow denote different benzene molecules. (B) Crystals of **2** have one-dimensional cavities that contain benzene molecules.

local near-coplanarity with adjacent macrocyclic pyrrole groups. The disposition of the trimethoxyphenyl groups to the adjacent pyrrole groups of the macrocycle remains similar to that in **1**. Thus, the two-electron oxidation of **1** results in considerable conformational changes so that, for instance, the dihedral angle subtended between the two quinoid moieties in **2** is reduced by 100° compared to that between phenol moieties in **1**. Such a mechanical deformation of a porphyrin macrocycle triggered by photoredox reaction has rarely been reported. A symptom of the macrocyclic deformation is illustrated in Figure 4. Molecules of **2** are packed in columnar arrays with benzene molecules included in the resulting tubular cavity. In fact, because quinonoid molecules (e.g., TCNQ) are known to form charge-transfer complexes with electron donors such as tetrathiafulvalene,[27] this aspect of **2** suggests its activity as an electron-accepting host molecule for charge-transfer complex formation.

To characterize the processes involved in converting **1** to **2** and *vice versa*, femtosecond transient absorption spectroscopy was used to investigate the intermediates of the photoredox cycle. During the forward photooxidation process (from **1** to **2**), absorption increases at 750 nm due to the singlet excited state of porphyrin $^1[\mathbf{1}^{2-}]^*$, with concurrent bleaching of the Q-band at 600 nm (Figure 5A). Under argon, $^1[\mathbf{1}^{2-}]^*$ relaxes within 100 ps to a triplet excited state $^3[\mathbf{1}^{2-}]^*$, and then $^3[\mathbf{1}^{2-}]^*$ relaxes to its ground state within 700 ps. In contrast, under aerobic conditions, electron transfer from $^3[\mathbf{1}^{2-}]^*$ to aerial O_2 occurs, yielding a porphyrin radical anion $\mathbf{1}^{\bullet-}$ with absorption at 450 and 600 nm (Figure 5B). Electron spin resonance (ESR) spectroscopy revealed formation of the phenoxy radical anion $\mathbf{1}^{\bullet-}$ (g = 2.0043) (Figure 6A). The simulated ESR spectrum indicates that this radical is coupled with two nonequivalent protons, presumably nearby methine protons of the phenoxy group, which may be nonequivalent due to a counterion (TBA^+ or F^-) interacting at the macrocyclic amine or imine groups. Additionally, on cooling of the sample to 77 K following photooxidation, the ESR spectrum contained a signal characteristic of the superoxide radical anion $O_2^{\bullet-}$ ($g_\parallel$ = 2.0909, $g_\perp$ = 2.0037), revealing that ambient O_2 acts as the oxidant.[22,28] Some of these observations are consistent with mechanisms of oxidation of phenol-substituted porphyrins reported in previous intensive investigations by Milgrom and co-workers.[11d,18c,18d,29] The important feature of redox behavior of phenol-substituted porphyrins is to identify

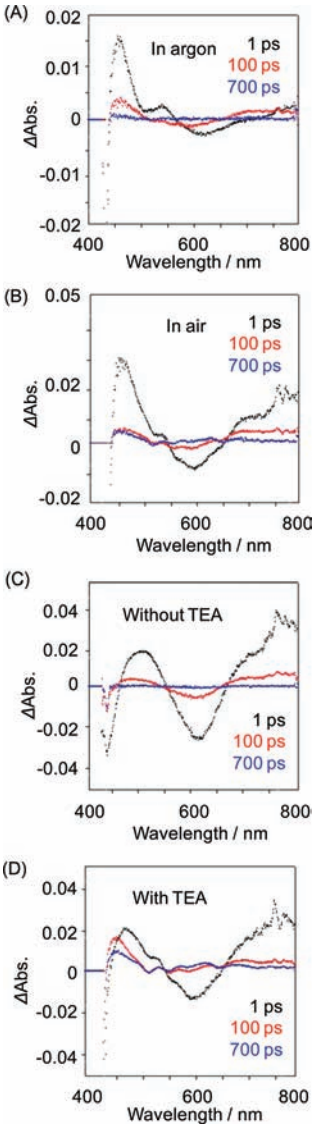

Figure 5. Transient absorption spectra (laser excitation at 430 nm, in CH_2Cl_2) of (A) $\mathbf{1}^{2-}$ in argon, (B) $\mathbf{1}^{2-}$ in air, (C) **2** without TEA, and (D) **2** with TEA. Spectra assigned as in our previous report.[6b]

the site of initial aerial oxidation (indicated by formation of characteristic radical species) and determine any subsequent electronic rearrangements, which might yield other information on excited-state species. These matters are critical in biochemical systems, where radical species are involved as intermediates in many processes, and may also involve phenol substituents such as tyrosyl moieties. According to Milgrom and co-workers, base-catalyzed aerial oxidation initially occurs by deprotonation of phenol moieties followed by a rapid one-electron oxidation, which gives rise to a solution whose ESR spectrum contains contributions from two species: a *meso*-substituent-centered radical anion and a porphyrin radical anion, which may be interchangeable on the ESR time scale.[18c] In the case we describe here, while both a substituent-centered radical and a porphyrin radical anion are observed, they do not appear to interchange under the conditions of the forward oxidation process. We believe that the substituent-centered radical resulting from the initial deprotonation/oxidation step is stabilized by the presence of

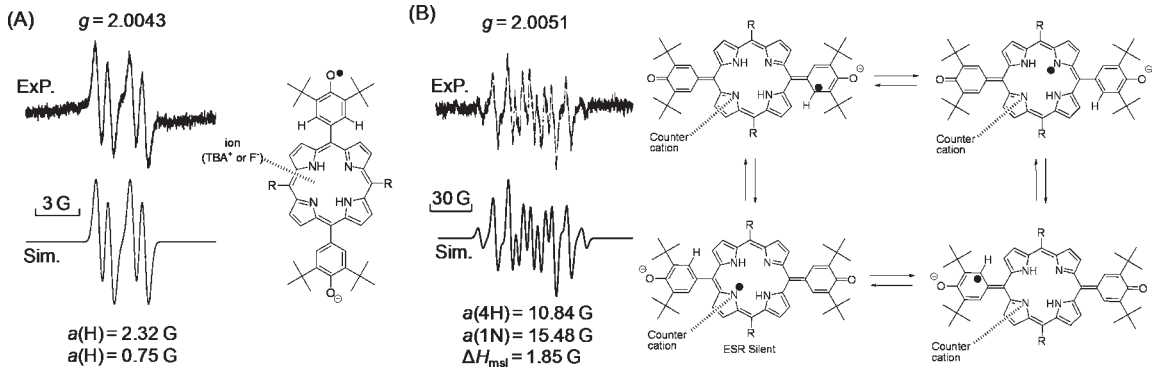

Figure 6. (A) Experimentally measured (ExP.) and simulated (Sim.) ESR spectra of (a) $\mathbf{1}^{2-}$ during photoirradiation by a high-pressure Hg lamp ($\lambda >$ 340 nm) under air ([**1**] = 0.33 mM, [F^-] = 0.1 M in CH_2Cl_2 at room temperature) and (B) **2** with TEA after photoirradiation at 430 nm under argon ([**2**] = 1.0 mM, [TEA] = 0.1 M in CH_2Cl_2 at room temperature). The *hfc* values (in gauss) used for the simulations are indicated on the structure of the radical anions, and those values were obtained from DFT calculations. ΔH_{msl} represents the maximum slope of line width used for simulations. R = 3,4,5-trimethoxyphenyl.

fluoride ions, which are known to interact with porphyrin NH groups,[19,20] thus preventing radical delocalization by reason of electrostatic repulsion and giving rise to a relatively simple four-line ESR spectrum. Conversely, during reduction, ionic species present in solution interact with the $\mathbf{2}^{\bullet-}$ species (whose radical is also delocalized), leading to lower symmetry and a complex, many-line ESR spectrum (see Figure 6B).

Femtosecond transient absorption spectroscopy was also applied to investigate the reverse photoreduction process (from **2** to **1**). The transient absorption spectrum at 1 ps increases at 750 nm due to the singlet excited state $^1[\mathbf{2}]^*$ with concurrent bleaching of the Q-band at 600 nm (Figure 5C). In the absence of TEA, the excited state relaxed within 700 ps. In contrast, in the presence of TEA, the singlet state $^1[\mathbf{2}]^*$ is quenched, resulting in formation of the radical anion $\mathbf{2}^{\bullet-}$ (Figure 5D). ESR spectroscopy supports the formation of radical anion $\mathbf{2}^{\bullet-}$ (g = 2.0051) (Figure 6B). Fitting of this ESR spectrum indicates that the radical is delocalized over quinonoid carbon and pyrrolic nitrogen atoms, where counter cations break the symmetry, leading to a complex ESR spectrum.[30] Thus, the radical species formed during forward and reverse processes differ in the localization of the unpaired electron density: oxidation of **1** occurs via a phenoxyl radical, while reduction of **2** occurs via a porphyrinic radical. This is a noteworthy feature of this system since the identity of the radical intermediate state is a characteristic determined by the direction of the chemical reaction; i.e., photoreduction (the reverse **2**→**1** reaction) is denoted by the presence of a porphyrinic radical.

Figure 7 shows energy level diagrams of photochemical processes, obtained by a combination of electrochemical measurements (cyclic voltammetry[22]) and spectroscopic measurements. In photooxidation of **1** (Figure 7A), its HOMO level, locating at 0.32 eV (vs Fc/Fc^+), is significantly reduced to −0.88 eV (vs Fc/Fc^+) by addition of F^-. However, the HOMO level of resultant $\mathbf{1}^{2-}$ is not sufficiently low to permit oxidization by ambient dioxygen (LUMO = −1.66 V, vs Fc/Fc^+). Photoirradiation of $\mathbf{1}^{2-}$ excites an electron to its LUMO level at −2.00 eV and causes the electron transfer from $\mathbf{1}^{2-}$ to oxygen, yielding $\mathbf{1}^{\bullet-}$. It is probable that two molecules of $\mathbf{1}^{\bullet-}$ undergo disproportionation to produce **1** and **2**, similar to the case reported by Milgrom during oxidation of 5,10,15,20-tetrakis(3,5-di-*tert*-butyl-4-hydroxyphenyl)porphyrin.[31] On the other hand, photoactivation of **2** produces an electron−hole at a HOMO level of 0.66 eV (vs Fc/Fc^+),

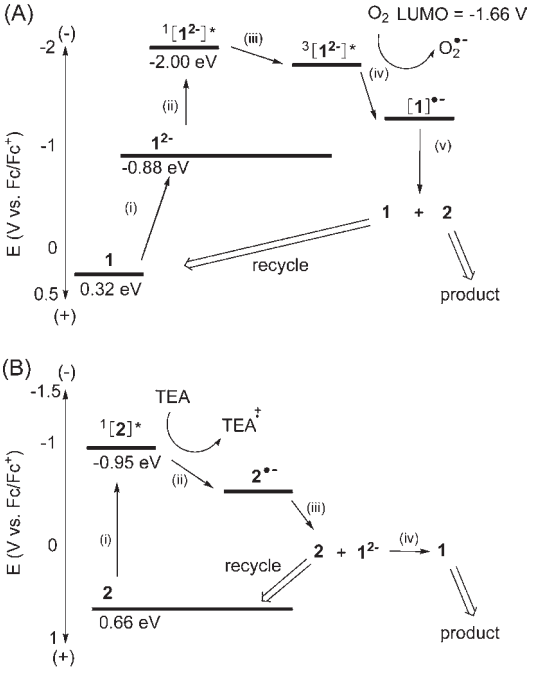

Figure 7. (A) Energy level diagrams for photooxidation of **1** into **2**: (i) TBAF, (ii) photoexcitation by UV, (iii) relaxation, (iv) electron transfer to O_2, and (v) disproportionation involving two radicals. (B) Energy level diagrams for photoreduction of **2** into **1**: (i) photoexcitation by white light, (ii) electron transfer from TEA, (iii) disproportionation, and (iv) protonation presumably by water or decomposed material from TEA. The energy levels have been estimated according to cyclic voltammetry, electronic absorption spectroscopy, and fluorescence measurements.

which is sufficient to produce $\mathbf{2}^{\bullet-}$ as a result of electron transfer from TEA to **2**. Thus, close matching of HOMO−LUMO energy levels is critical in the design and preparation of photoredox phenol-substituted porphyrins.

CONCLUSION

In conclusion, we present here a chimeric porphyrin−hydroquinone hybrid which combines the photonic functionality of porphyrins with the redox activity of hydroquinones. The

amalgamation of porphyrin and hydroquinone molecular archetypes yields a new form of photoredox-active molecule, which undergoes considerable but reversible variation of its electronic and physical structures under appropriate photochemical conditions. Our molecular design indicates a simple and versatile method for producing photoredox macrocyclic compounds, which could lead to a new class of advanced functional materials suitable for bottom-up fabrication of molecular devices and machines. The characteristics of this system illustrate not only that it is possible to combine the properties of different chemical entities (as has been previously shown) but also that the oxidation state can be strongly coupled with the physical structure of the molecule—an important feature for the development of molecular-scale devices.

EXPERIMENTAL SECTION

Materials. Pyrrole, 3,5-di-*tert*-butyl-4-hydroxybenzaldehyde, 3,4,5-trimethoxybenzaldehyde, and tetra-*n*-butylammonium fluoride (all from Tokyo Chemical Industry Co.), and propionic acid and triethylamine (both from Kanto Chemical Co.), were used as received. Dehydrated dichloromethane (Wako Pure Chem. Co.) was used for spectroscopic measurements. Solvents for NMR spectroscopic measurements were purchased from Cambridge Isotope Laboratories Inc. Dehydrated *o*-dichlorobenzene (Aldrich Chemical Co.) and tetra-*n*-butylammonium perchlorate (Nakalai Tesque) were used for cyclic voltammetry without purification. Porphyrin **3** (the non-methoxylated analogue of **1**) was prepared as previously reported.[5]

General Methods. All ^{1}H NMR spectra were obtained at 298 K (unless otherwise stated) using an AL300 BX spectrometer (JEOL, Tokyo, Japan). Mass spectra were measured using a Shimadzu-Kratos Axima CFR+ MALDI−TOF mass spectrometer with dithranol as matrix. High-resolution mass spectra (FAB positive-ion mode, Xe) were obtained using a JMS-SX102A mass spectrometer (JEOL) with 3-nitrobenzyl alcohol as matrix. Electronic absorption spectra were measured using a Shimadzu UV-3600 UV-vis-NIR spectrophotometer at room temperature. Fluorescence emission spectra were obtained with a JASCO FP-6500 spectrofluorometer at room temperature under air.

Synthesis of 1. Pyrrole (6.71 g, 0.100 mol) was added to a solution of 3,5-di-*tert*-butyl-4-hydroxybenzaldehyde (2.34 g, 0.0500 mol) and 3,4,5-trimethoxybenzaldehyde (1.96 g, 0.0500 mol) in refluxing propionic acid (500 mL) with stirring. The solution was subsequently refluxed for 2 h. The reaction mixture was then reduced to approximately half its volume under reduced pressure and allowed to cool to room temperature. Methanol (250 mL) was added, and the resulting purple precipitate was collected by filtration and washed copiously with methanol. The crude product was subjected to column chromatography (SiO_2, CH_2Cl_2/hexane = 1/1). The third band eluting from the column was collected and evaporated to dryness. The product was dried *in vacuo* to afford **1** as a purple powder (500 mg, 1.9%). ^{1}H NMR ($CDCl_3$, 300 MHz, 20 °C): δ = 8.94 (s, 8H, pyrrole β-H), 8.04 (s, 4H, Ar−H), 7.49 (s, 4H, Ar−H), 5.54 (s, 2H, Phenol−OH), 4.17 (s, 6H, OCH_3), 3.97 (s, 12H, OCH_3), 1.63 (s, 36H, *t*-Bu), −2.69 (s, 2H, inner-NH) ppm. ^{13}C NMR ($CDCl_3$, 300 MHz, 20 °C): δ = 153.9, 151.5, 138.2, 134.3, 133.3, 132.2, 121.8, 119.7, 113.0, 61.5, 56.6, 34.9, 30.8 ppm. ESI-TOF-MS: m/z 1051.56 $[M+H]^+$. HRMS: calcd for $C_{66}H_{74}N_4O_8$ 1050.5507, found 1050.5513. Mp >200 °C.

Large-Scale Synthesis of 2. A large excess of TBAF (2.0 g, 7.2 mmol) was added to a stirred solution of porphyrin **1** (50 mg, 0.048 mmol) in CH_2Cl_2 (200 mL). The dark red solution was irradiated at room temperature with ultraviolet light from a mercury lamp (365 nm). After 1 h of irradiation, the solution had changed color to dark green. The solution was washed with H_2O twice to remove TBAF and then dried over Na_2SO_4. The solvent was evaporated under reduced pressure, and the residue was subjected to column silica gel chromatography (SiO_2, CH_2Cl_2/hexane = 1/1). The green fraction was collected, and solvents were evaporated. Recrystallization from benzene under hexane atmosphere afforded **2** (38 mg, 76%) as dark green block crystals. ^{1}H NMR ($CDCl_3$, 300 MHz, 20 °C): δ = 7.63 (s, 4H, Ar-H), 6.78 (s, 4H, Ar-H), 6.73 (d, 4H, pyrrole β-H, J = 7.0 Hz), 6.80 (d, 4H, pyrrole β-H, J = 7.0 Hz), 3.95 (s, 6H, OCH_3), 3.89 (s, 12H, OCH_3), 1.28 (s, 36H, *t*-Bu) ppm. ^{13}C NMR ($CDCl_3$, 300 MHz, 20 °C): δ = 152.4, 148.6, 142.2, 141.6, 132.1, 130.0, 128.9, 122.8, 108.4, 60.9, 56.2, 35.6, 29.5 ppm. ESI-TOF-MS: m/z 1049.54 $[M+H]^+$. HRMS: calcd for $C_{66}H_{72}N_4O_8$ 1049.2999, found 1050.5465. Note that HRMS of **2** causes laser-induced reduction to **1**. Mp >200 °C.

Photooxidation of 1. A solution of **1** (2.3×10^{-5} M, 5 mL) in dry CH_2Cl_2 was added to excess (more than 100 equiv) solid TBAF hydrate. The solution was irradiated with ultraviolet light (365 nm) under ambient atmosphere, and the progress of the photoreaction was monitored by using UV-vis spectrophotometry. After 5 min, the solution was washed with H_2O and then dried over anhydrous Na_2SO_4.

Photoreduction of 2. A solution of **2** (2.3×10^{-5} M, 3 mL) in CH_2Cl_2 was added to TEA (100 μL). The solution was degassed using freeze−pump−thaw cycles under argon, and then the solution was irradiated with white light (300 nm−760 nm). The progress of the photoreaction was monitored by using UV-vis spectrophotometry.

X-ray Crystallography. Diffraction data for **1** (crystallized by diffusion of hexane into a dichloromethane solution of **1**) and **2** (crystallized by diffusion of hexane into their respective benzene solutions) were collected at 160 K using a Bruker APEX CCD diffractometer using graphite-monochromated Mo Kα radiation. Diffraction data for $\mathbf{3}^{2-}$ (crystallized by diffusion of tetrahydrofuran into a dichloromethane solution of $\mathbf{3}^{2-}$) and **4** (crystallized by diffusion of hexane into a benzene solution of **3**) were collected using a Bruker APEX 2 CCD diffractometer at 150 K for $\mathbf{1}^{2-}$ and 100 K for **3** using silicon 111 monochromated synchrotron radiation at ALS station 11.3.1.[32a] Structure solutions were by direct methods, and refinement was with SHELXTL.[32]

Femtosecond Laser Flash Photolysis. Femtosecond laser flash photolysis was conducted as reported previously[33] by using an ultrafast source (Integra-C, Quantronix Corp.), an optical parametric amplifier (TOPAS, Light Conversion Ltd.), and a commercially available optical detection system (Helios, Ultrafast Systems LLC). The source for the pump and probe pulses was derived from the fundamental output of Integra-C (780 nm, 2 mJ/pulse, and fwhm =130 fs) at a repetition rate of 1 kHz. All experiments were performed at 298 K.

ESR Spectroscopy. ESR spectra were recorded by using a JEOL JESME-LX X-band spectrometer at room temperature with photoirradiation from a USHIO USH1005D high-pressure mercury lamp (1000 W) equipped with a water filter to remove infrared light and a cutoff glass filter (λ < 340 nm). ESR sample tubes (4.5 mm) charged with the samples were degassed and sealed under Ar. ESR measurements were performed under nonsaturating microwave power conditions. The amplitude of modulation was chosen to optimize the resolution and the signal-to-noise ratio of the observed spectra. The Calleo ESR program[34] was used for simulations of ESR spectra to determine the hyperfine coupling constants.

Cyclic Voltammetry. Cyclic voltammetry and differential pulse voltammetry were carried out on argon-saturated *o*-dichlorobenzene solutions containing *n*-Bu_4NClO_4 (0.1 M) by using a 612B ALS/HCH electrochemical analyzer (ALS) with a conventional three-electrode cell. Glassy carbon disk (diameter 3.0 mm, working), Pt wire (counter), and $Ag/Ag^+/CH_3CN$/*n*-Bu_4NClO_4 (reference) electrodes were used. All potentials are quoted relative to the Fc/Fc^+ redox couple.

ASSOCIATED CONTENT

Supporting Information. Experimental details and additional data, including CIF files for **1**, **2**, $\mathbf{3}^{2-}$, and **4**. This material is available free of charge via the Internet at http://pubs.acs.org.

AUTHOR INFORMATION

Corresponding Author
jonathan.hill@nims.go.jp; ariga.katsuhiko@nims.go.jp

ACKNOWLEDGMENT

This research was partially supported by the World Premier International (WPI) Research Center Initiative on Materials Nanoarchitectonics and Grant-in-Aid (No. 20108010) from MEXT (Japan), Core Research for Evolutional Science and Technology (CREST) from JST (Japan), and KOSEF/MEST through the WCU project (R31-2008-000-10010-0). A.S. and J.L. are grateful to Japan Society for Promotion of Science (JSPS) for Fellowships. Advanced Light Source (ALS) is supported by the Director, Office of Science, Office of Basic Energy Sciences, of the U.S. Department of Energy under Contract No. DE-AC02-05CH11231. Dr. Toshimichi Shibue, Mr. Natsuhiko Sugimura, and Mrs. Asami Urazoe (Waseda University) are acknowledged for high-resolution mass spectrometry.

REFERENCES

(1) (a) Wasielewski, M. R. *Chem. Rev.* **1992**, *92*, 435. (b) Meyer, T. J. *Acc. Chem. Res.* **1989**, *22*, 163. (c) Gust, D.; Moore, T. A.; Moore, A. L. *Acc. Chem. Res.* **2001**, *34*, 40. (d) Drain, C. M.; Gentemann, S.; Roberts, J. A.; Nelson, N. Y.; Medforth, C. J.; Jia, S.; Simpson, M. C.; Smith, K. M.; Fajer, J.; Shelnutt, J. A.; Holten, D. *J. Am. Chem. Soc.* **1998**, *120*, 3781. (e) Imahori, H.; Tamaki, K.; Guldi, D. M.; Luo, C.; Fujitsuka, M.; Ito, O.; Sakata, Y.; Fukuzumi, S. *J. Am. Chem. Soc.* **2001**, *123*, 2607. (f) Imahori, H.; Guldi, D. M.; Tamaki, K.; Yoshida, Y.; Luo, C.; Sakata, Y.; Fukuzumi, S. *J. Am. Chem. Soc.* **2001**, *123*, 6617.

(2) Miller, J. S.; Epstein, A. J. *Angew. Chem., Int. Ed. Engl.* **1994**, *33*, 385.

(3) Collman, J. P.; Wagenknecht, P. S.; Hutchison, J. E. *Angew. Chem., Int. Ed. Engl.* **1994**, *33*, 1537.

(4) (a) Balaban, T. S. *Acc. Chem. Res.* **2005**, *38*, 612. (b) Drain, C. M.; Varotto, A.; Radivojevic, I. *Chem. Rev.* **2009**, *109*, 1630. (c) Beletskaya, I.; Tyurin, V. S.; Tsivadze, A. Y.; Guilard, R.; Stern, C. *Chem. Rev.* **2009**, *109*, 1659. (d) Tomohiro, Y.; Satake, A.; Kobuke, Y. *J. Org. Chem.* **2001**, *66*, 8442. (e) Cheng, K. F.; Drain, C. M.; Grohmann, K. *Inorg. Chem.* **2003**, *42*, 2075.

(5) Shundo, A.; Hill, J. P.; Ariga, K. *Chem.—Eur. J.* **2009**, *15*, 2486.

(6) (a) Hill, J. P.; Schmitt, W.; McCarty, A. L.; Ariga, K.; D'Souza, F. *Eur. J. Org. Chem.* **2005**, 2893. (b) D'Souza, F.; Subbaiyan, N. K.; Xie, Y.; Hill, J. P.; Ariga, K.; Ohkubo, K.; Fukuzumi, S. *J. Am. Chem. Soc.* **2009**, *131*, 16138. (c) Jose, D. A.; Shukla, A. D.; Kumar, D. K.; Ganguly, B.; Das, A. *Inorg. Chem.* **2005**, *44*, 2414.

(7) (a) Kamo, M.; Tsuda, A.; Nakamura, Y.; Aratani, N.; Furukawa, K.; Kato, T.; Osuka, A. *Org. Lett.* **2003**, *5*, 2079. (b) Hayashi, S.; Sung, J.; Sung, Y. M.; Inokuma, Y.; Kim, D.; Osuka, A. *Angew. Chem., Int. Ed.* **2011**, *50*, 3253.

(8) (a) Blake, I. M.; Anderson, H. L.; Beljonne, D.; Brédas, J.-L.; Clegg, W. *J. Am. Chem. Soc.* **1998**, *120*, 10764. (b) Blake, I. M.; Krivokapic, A.; Katterle, M.; Anderson, H. L. *Chem. Commun.* **2002**, 1662.

(9) (a) Fukuda, T.; Masuda, S.; Kobayashi, N. *J. Am. Chem. Soc.* **2007**, *129*, 5472. (b) Fukuda, T.; Hashimoto, N.; Araki, Y.; El-Khouly, M. E.; Ito, O.; Nagao, N. *Chem.—Asian J.* **2009**, *4*, 1678. (c) D'Souza, F.; Chitta, R.; Ohkubo, K.; Tasior, M.; Subbaiyan, N. K.; Zandler, M. E.; Rogacki, M.; Gryko, D. T.; Fukuzumi, S. *J. Am. Chem. Soc.* **2008**, *130*, 14263. (d) Maligaspe, E.; D'Souza, F. *Org. Lett.* **2010**, *12*, 624. (e) Xie, Y.; Hill, J. P.; Schumacher, A. L.; Sandanayaka, A. S. D.; Araki, Y.; Karr, P. A.; Labuta, J.; D'Souza, F.; Ito, O.; Anson, C. E.; Powell, A. K.; Ariga, K. *J. Phys. Chem. C* **2008**, *112*, 10559.

(10) Kadish, K. M.; E, W.; Zhan, R.; Khoury, T.; Govenlock, L. J.; Prashar, J. K.; Sintic, P. J.; Ohkubo, K.; Fukuzumi, S.; Crossley, M. J. *J. Am. Chem. Soc.* **2007**, *129*, 6576.

(11) (a) Fuhrhop, J.-H.; Besecke, S.; Subramanian, J.; Mengersen, C.; Riesner, D. *J. Am. Chem. Soc.* **1975**, *97*, 7141. (b) Fuhrhop, J.-H.; Baumgartner, E.; Bauer, H. *J. Am. Chem. Soc.* **1981**, *103*, 5854. (c) Melezhik, A. V.; Pokhodenko, V. D. *Zh. Org. Khim.* **1982**, *18*, 1054. (d) Milgrom, L. R. *Tetrahedron* **1983**, *39*, 3895. (e) Traylor, T. G.; Nolan, K. B.; Hildreth, R. *J. Am. Chem. Soc.* **1983**, *105*, 6149. (f) Evans, T. A.; Srivatsa, G. S.; Sawyer, D. T.; Traylor, T. G. *Inorg. Chem.* **1985**, *24*, 4733. (g) Balch, A. L.; Noll, B. C.; Reid, S. M.; Zovinka, E. P. *Inorg. Chem.* **1993**, *32*, 2610. (h) Wojaczynski, J.; Latos-Grazynski, L. *Inorg. Chem.* **1995**, *34*, 1044.

(12) Xie, Y.; Hill, J. P.; Schumacher, A. L.; Karr, P. A.; D'Souza, F.; Anson, C. E.; Powell, A. K.; Ariga, K. *Chem.—Eur. J.* **2007**, *13*, 9824.

(13) Oh, M.; Carpenter, G. B.; Sweigart, D. A. *Acc. Chem. Res.* **2004**, *37*, 1.

(14) (a) Grier, D. G. *Nature* **2003**, *424*, 811. (b) Irie, M.; Fukaminato, T.; Sasaki, T.; Tamai, N.; Kawai, T. *Nature* **2002**, *420*, 759. (c) Hugel, T.; Holland, N. B.; Cattani, A.; Moroder, L.; Seitz, M.; Gaub, H. E. *Science* **2002**, *296*, 1103. (d) Tamai, N.; Miyasaka, H. *Chem. Rev.* **2000**, *100*, 1875. (e) Heilemann, M.; Van de Linde, S.; Schuttpelz, M.; Kasper, R.; Seefeldt, B.; Mukherjee, A.; Tinnefeld, P.; Sauer, M. *Angew. Chem., Int. Ed.* **2008**, *47*, 6172. (f) Heilemann, M.; Dedecker, P.; Hofkens, J.; Sauer, M. *Laser Photon. Rev.* **2009**, *3*, 180. (g) Zhuang, X. *Nat. Photonics* **2009**, *3*, 365.

(15) (a) Hell, S. W. *Nat. Biotechnol.* **2003**, *21*, 1347. (b) Barnes, W. L.; Dereux, A.; Ebbesen, T. W. *Nature* **2003**, *424*, 824.

(16) (a) Special issue on Photochromism: Memories and Switches, Irie, M., Ed. *Chem. Rev.* **2000**, *100*, 1683. (b) Browne, W. R.; Feringa, B. L. *Nat. Nanotechnol.* **2006**, *1*, 25. (c) Retsek, J. L.; Drain, C. M.; Kirmaier, C.; Nurco, D. J.; Medforth, C. J.; Smith, K. M.; Sazanovich, I. V.; Chirvony, V. S.; Fajer, J.; Holten, D. *J. Am. Chem. Soc.* **2003**, *125*, 9787. (d) Saha, S.; Stoddart, J. F. *Chem. Soc. Rev.* **2007**, *36*, 77. (e) Kay, E. R.; Leigh, D. A.; Zerbetto, F. *Angew. Chem., Int. Ed.* **2007**, *46*, 72. (f) Kobatake, S.; Takami, S.; Muto, H.; Ishikawa, T.; Irie, M. *Nature* **2007**, *446*, 778. (g) Ikeda, T.; Mamiya, J.; Yu, Y. *Angew. Chem., Int. Ed.* **2007**, *46*, 506. (h) Ariga, K.; Hill, J. P.; Lee, M. V.; Vinu, A.; Charvet, R.; Acharya, S. *Sci. Technol. Adv. Mater.* **2008**, *9*, 014109. (i) Yagai, S.; Kitamura, A. *Chem. Soc. Rev.* **2008**, *37*, 1520. (j) Browne, W. R.; Feringa, B. L. *Annu. Rev. Phys. Chem.* **2009**, *60*, 407.

(17) (a) Tsivgoulis, G. M.; Lehn, J.-M. *Angew. Chem., Int. Ed. Engl.* **1995**, *34*, 1119. (b) Kawai, S. H.; Gilat, S. L.; Ponsinet, R.; Lehn, J.-M. *Chem.—Eur. J.* **1995**, *1*, 285.

(18) (a) Nishide, H.; Yoshioka, N.; Inagaki, K.; Tsuchida, E. *Macromolecules* **1988**, *21*, 3119. (b) Nishide, H.; Yoshioka, N.; Inagaki, K.; Kaku, T.; Tsuchida, E. *Macromolecules* **1992**, *25*, 569. (c) Milgrom, L. R.; Hill, J. P.; Flitter, W. D. *J. Chem. Soc., Perkin Trans. 2* **1994**, *3*, 521. (d) Milgrom, L. R.; Hill, J. P.; Flitter, W. D. *J. Chem. Soc., Chem. Commun.* **1992**, *10*, 773.

(19) (a) Braun, J.; Hasenfratz, C.; Schwesinger, R.; Limbach, H.-H. *Angew. Chem., Int. Ed. Engl.* **1994**, *33*, 2215. (b) Braun, J.; Schwesinger, R.; Williams, P. G.; Morimoto, H.; Wemmer, D. E.; Limbach, H.-H. *J. Am. Chem. Soc.* **1996**, *118*, 11101.

(20) Takeuchi, M.; Shioya, T.; Swager, T. M. *Angew. Chem., Int. Ed.* **2001**, *40*, 3372.

(21) Crystal data for **1**: $C_{66}H_{74}N_4O_8 \cdot CH_2Cl_2$, FW = 1136.25 g/mol, monoclinic, $P2_1/n$, a = 15.102(4) Å, b = 14.324(3) Å, c = 15.194(4) Å, α = 90.00°, β = 92.847(4)°, γ = 90.00°, V = 3282.8(13) Å^3, Z = 2, ρ_{calc} = 1.079 g/cm^3, $R1$ = 0.0512, w$R2$ = 0.1355. Crystal data for **2**: $C_{66}H_{72}N_4O_8 \cdot 2C_6H_6$, FW = 1205.52 g/mol, triclinic, $P\bar{1}$, a = 14.677(4) Å, b = 14.833(4) Å, c = 17.768(5) Å, α = 111.834(4)°, β = 91.375(4)°, γ = 113.717(4)°, V = 3218.12 Å^3, Z = 2, ρ_{calc} = 1.017 g/cm^3, $R1$ = 0.0667, w$R2$ = 0.1833. Crystal data for for $\mathbf{3}^{2-}$: $C_{106}H_{160}N_6O_{5.5}$, FW = 1606.40 g mol^{-1}, orthorhombic, $Pca2_1$, a = 19.3034(8) Å, b = 11.7118(4) Å, c = 43.8395(17) Å, V = 9911.1(7) Å^3, Z = 4, ρ_{calc} = 1.077 g m^{-3}, μ = 0.065 mm^{-1}, $R1$ = 0.0978, w$R2$ = 0.2651. CCDC files 807568 (**1**), 807569 (**2**), 807569 ($\mathbf{3}^{2-}$), and 807571 (**4**) contain the crystallographic data (also provided as in CIF format in theSupporting Information); these data can be obtained free of charge from The Cambridge Crystallographic Data Centre at www.ccdc.cam.ac.uk/data_request/cif.

(22) See Supporting Information.
(23) (a) Gale, P. A.; Sessler, J. L.; Kral, V.; Lynch, V. *J. Am. Chem. Soc.* **1996**, *118*, 5140. (b) Hill, J. P.; Schumacher, A. L.; D'Souza, F.; Labuta, J.; Redshaw, C.; Elsegood, M. J. R.; Aoyagi, M.; Nakanishi, T.; Ariga, K. *Inorg. Chem.* **2006**, *45*, 8288.
(24) White light was used for promoting the reduction process since light of discrete wavelengths (300−760 nm) was less effective for induction of photoreaction. However, transient absorption spectroscopy was performed under irradiation using laser light of 430 nm wavelength.
(25) X-ray crystal structures of the non-methoxy-substituted analogue of **2** (compound **4**) are shown in the Supporting Information. For typical structures of tetraphenylporphyrins, see: (a) Silvers, S. J.; Tulinsky, A. *J. Am. Chem. Soc.* **1967**, *89*, 3331. (b) Hökelek, T.; Ülkü, D. *Acta Crystallogr.* **1993**, *C49*, 1667.
(26) (a) Senge, M. O.; Runge, S.; Speck, M.; Ruhlandt-Senge, K. *Tetradedron* **2000**, *56*, 8927. (b) Botulinski, A.; Buchler, J. W.; Lee, Y. J.; Scheidt, W. R. *Inorg. Chem.* **1988**, *27*, 927.
(27) Bryce, M. R. *Chem. Soc. Rev.* **1991**, *20*, 355.
(28) (a) Bagchi, R. N.; Bond, A. M.; Scholz, F.; Stösser, R. *J. Am. Chem. Soc.* **1989**, *111*, 8270. (b) Fukuzumi, S.; Patz, M.; Suenobu, T.; Kuwahara, Y.; Itoh, S. *J. Am. Chem. Soc.* **1999**, *121*, 1605. (c) Fukuzumi, S.; Ohkubo, K. *Chem.—Eur. J.* **2000**, *6*, 4532. (d) Ohkubo, K.; Menon, S. C.; Orita, A.; Otera, J.; Fukuzumi, S. *J. Org. Chem.* **2003**, *68*, 4720.
(29) (a) Chan, A. C.; Dalton, J.; Milgrom, L. R. *J. Chem. Soc., Perkin Trans. 2* **1982**, 707. (b) Milgrom, L. R.; Mofidi, N.; Harriman, A. *J. Chem. Soc., Perkin Trans. 2* **1989**, 805. (c) Milgrom, L. R.; Flitter, W. D.; Short, E. L. *J. Chem. Soc., Chem. Commun.* **1991**, 788. (d) Milgrom, L. R.; Flitter, W. D. *J. Chem. Soc., Chem. Commun.* **1991**, 1492. (e) Golder, A. J.; Milgrom, L. R.; Nolan, K. B.; Povey, D. C. *J. Chem. Soc., Chem. Commun.* **1989**, 1751. (f) Milgrom, L. R.; Mofidi, N.; Jones, C. C.; Harriman, A. *J. Chem. Soc., Perkin Trans. 2* **1989**, 301. (g) Milgrom, L. R.; Yahioglu, G.; Jogiya, N. N. *Free Radical Res.* **1996**, *24*, 19.
(30) E, W.; Kadish, K. M.; Sintic, P. J.; Khoury, T.; Govenlock, L. J.; Ou, Z.; Shao, J.; Ohkubo, K.; Reimers, J. R.; Fukuzumi, S.; Crossley, M. J. *J. Phys. Chem. A* **2008**, *112*, 556.
(31) Milgrom, L. R.; Jones, C. C.; Harriman, A. *J. Chem. Soc., Perkin Trans. 2* **1988**, 71.
(32) (a) *SMART* (1997, 2001), *SAINT* (2001, 2008), and *APEX 2* (2008) software for CCD diffractometers. Bruker AXS Inc.: Madison, WI. (b) Sheldrick, G. M. *SHELXTL 5.1* (or *SHELTL 6.12*); Bruker AXS Inc.: Madison, WI, 1997 (2001). (c) Sheldrick, G. M. *Acta Crystallogr.* **2008**, *A64*, 112.
(33) Ohkubo, K.; Garcia, R.; Sintic, P. J.; Khoury, T.; Crossley, M. J.; Kadish, K. M.; Fukuzumi, S. *Chem.—Eur. J.* **2009**, *15*, 10493.
(34) *Calleo ESR*, Version 1.2; Calleo Scientific Software Publishers: Fort Collins, CO, 1996.